Hybrid photoluminescent material of lanthanide fluoride and graphene oxide with stronger luminescence intensity as chemical sensor of mercury ion

Richa Singhaal, Lobzang Tashi, Swaita Devi, Haq Nawaz Sheikh*

[a]Department of Chemistry, University of Jammu, Baba Sahib Ambedkar Road, Jammu-180006, India

(Supplementary Information)

Table of Contents

CONTENTS **Pages**

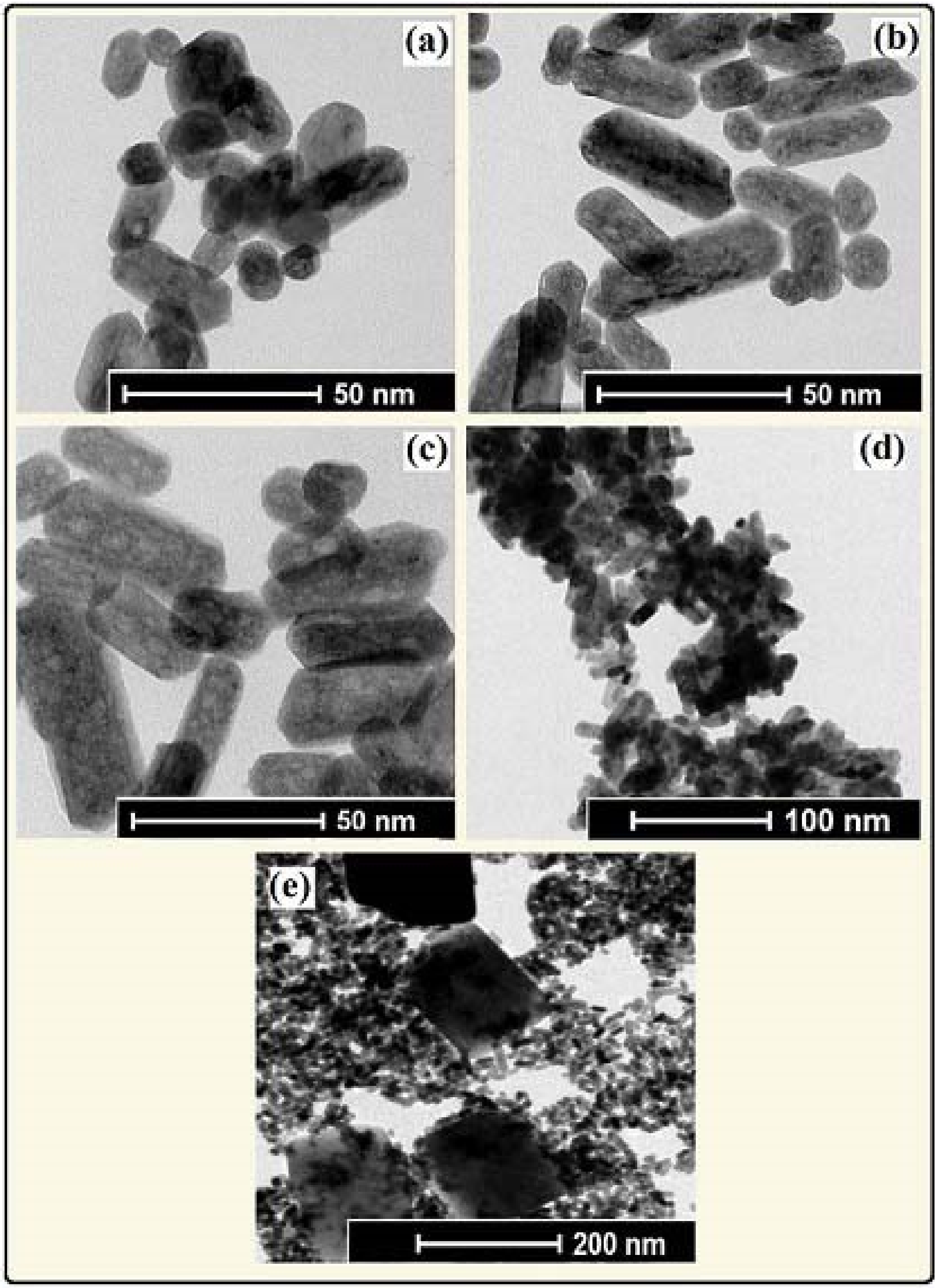

Fig. S1†: ESI TEM micrographs depicting the variations in the morphology of $Na_xLi_yGdF_4:Tb^{3+}$ nanoparticles at different Li/Na ions concentrations: where x/y = (a) x=15 mmol y= 0 mmol (b) x=10 mmol, y=5mmol (c) x=7.5 mmol y=7.5mmol (d) x=5mmol, y=10 mmol (e) x=0 mmol, y=15mmol.

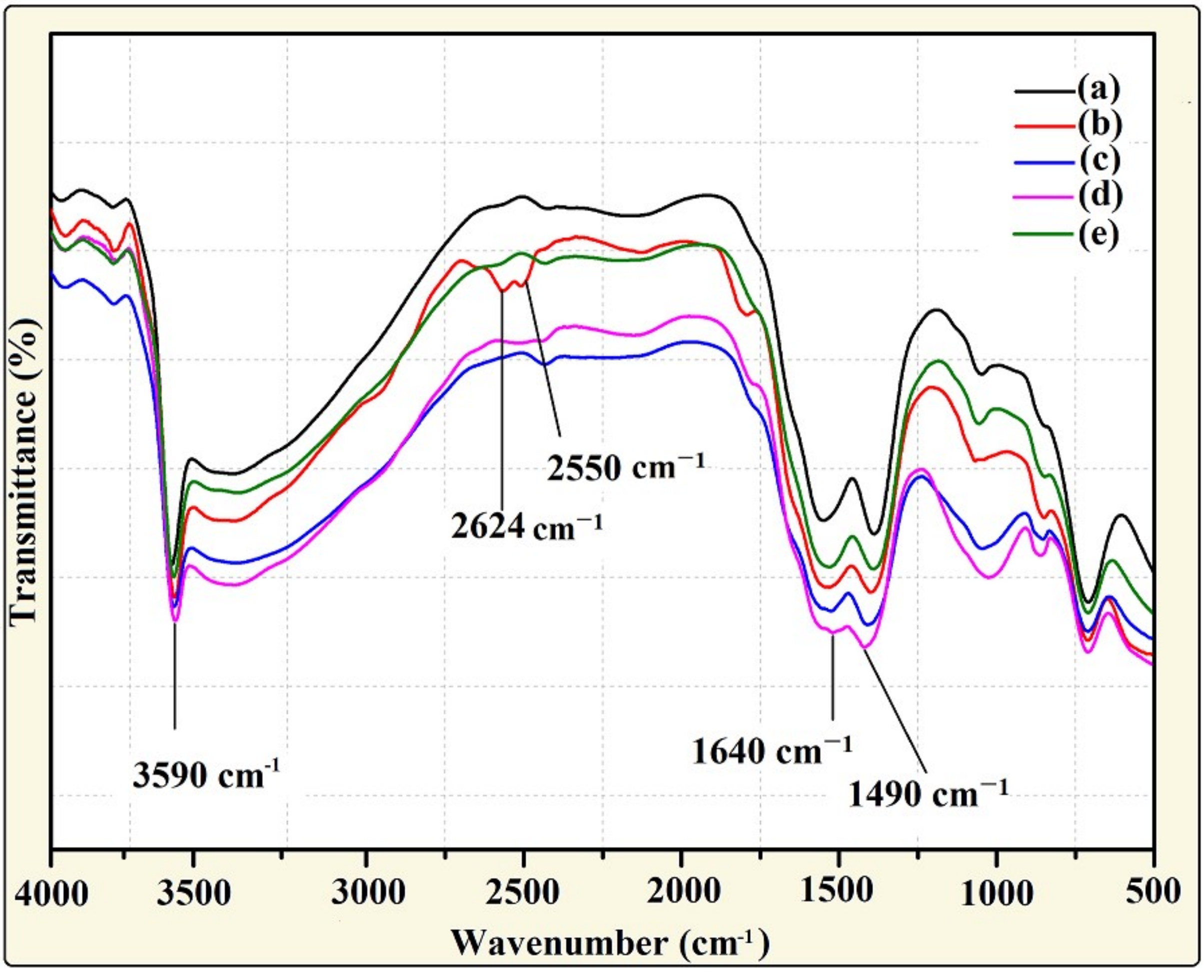

Fig. S2†: ESI FT-IR spectra visualizing the effect of different Na/Li ions concentrations on the **$Na_xLi_yGdF_4$:Tb^{3+}** nanophosphors **(a)** x=15 mmol y= 0 mmol **(b)** x=10 mmol, y=5mmol **(c)** x=7.5 mmol y=7.5mmol **(d)** x=5mmol, y=10 mmol **(e)** x=0 mmol, y=15mmol

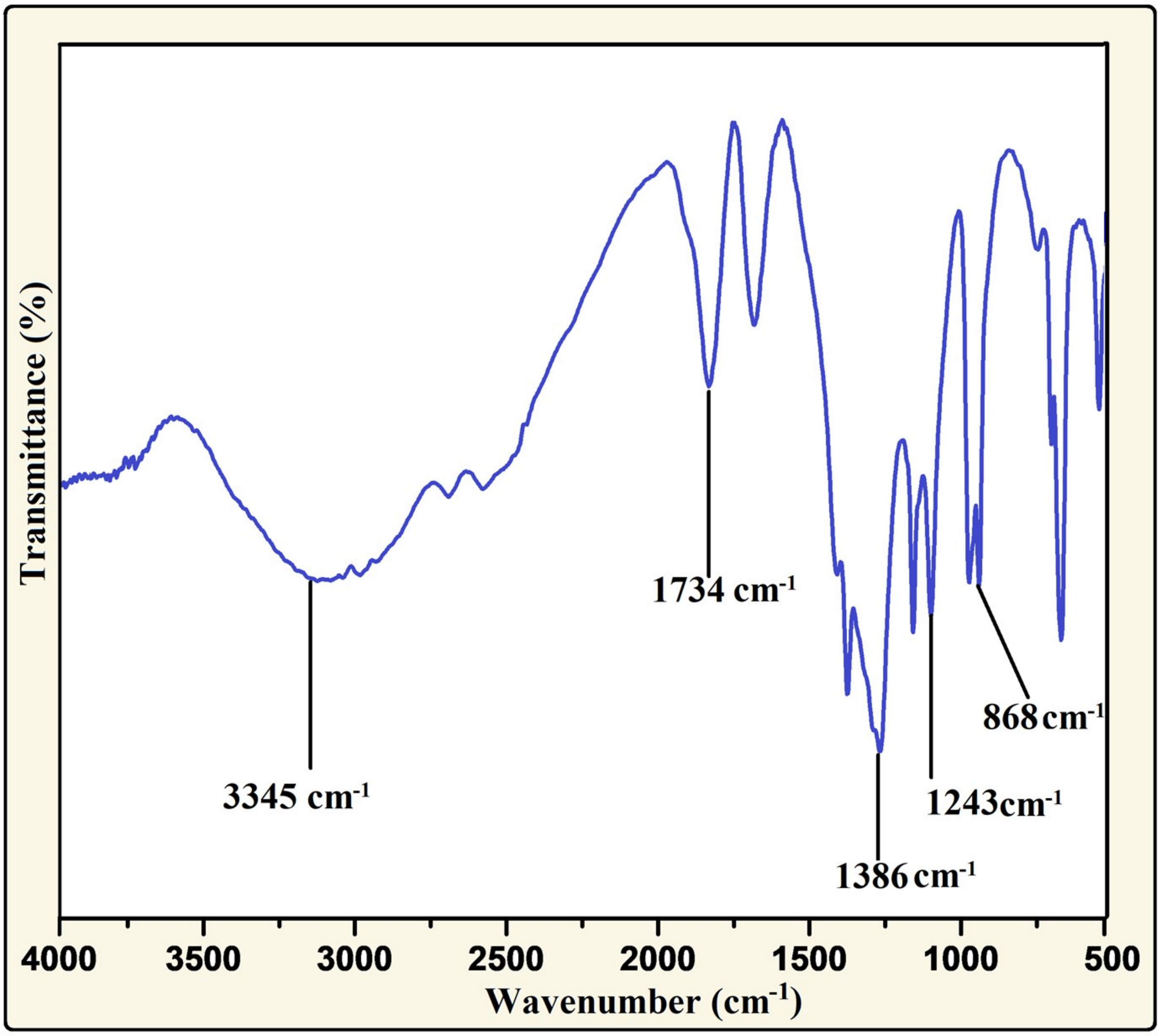

Fig. S3†: ESI FT-IR spectra of synthesized graphene oxide (GOSs)

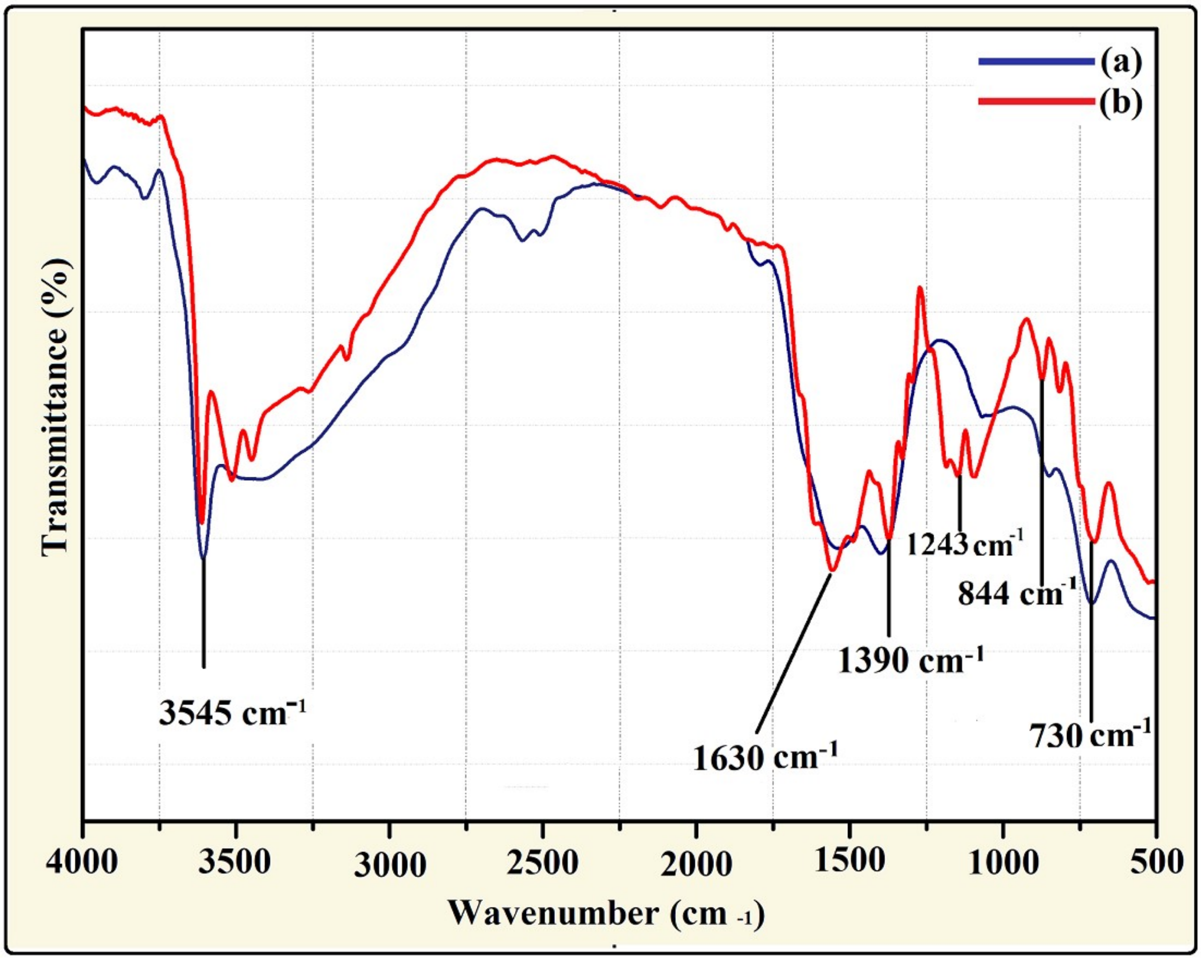

Fig. S4†: ESI FT-IR images displaying the presence of different functional groups attached to the synthesized nanostructure. **(a)** $Na_{10}Li_5GdF_4:Tb^{3+}$ nanophosphors. **(b)** $Na_{10}Li_5GdF_4:Tb^{3+}$@PMA@ Phen@ GO.

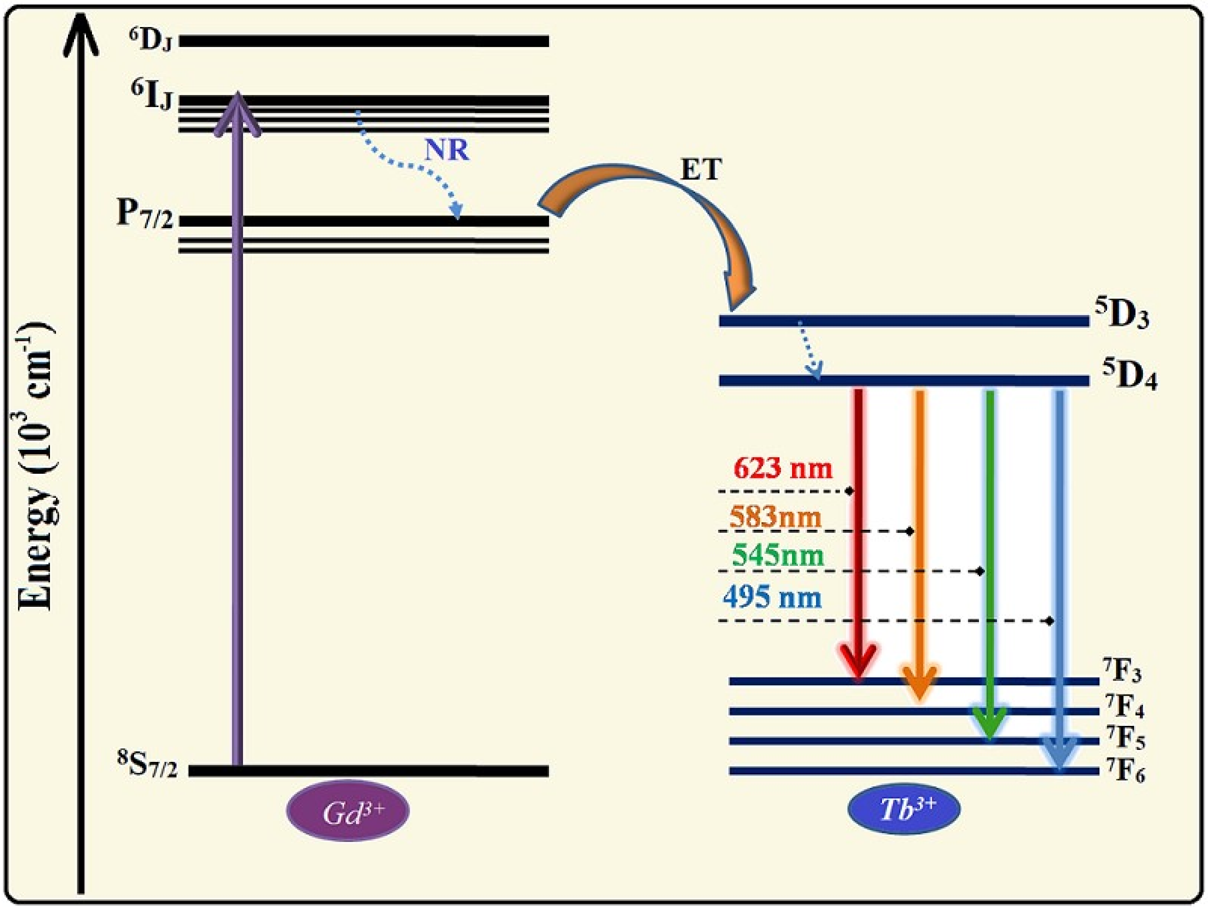

Fig. S5†: ESI Energy level diagram of as-synthesized $Na_xLi_yGdF_4:Tb^{3+}$nanophosphors showing efficient energy transfer from Gd^{3+} to Tb $^{3+}$ ions

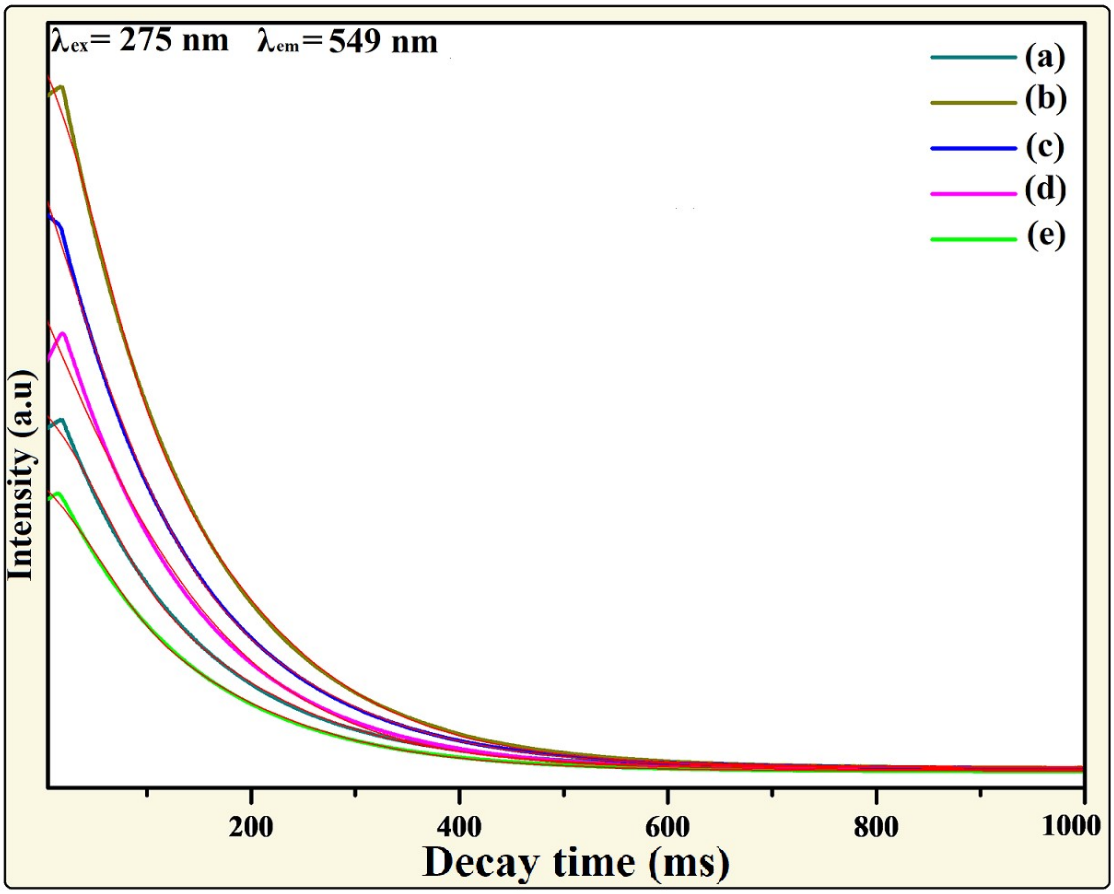

Fig. S6†: ESI Lifetime decay curve of as synthesized $Na_xLi_yGdF_4:Tb^{3+}$ nanophosphors at varying Na/Li ions concentrations **(a)** x=10 mmol y= 5 mmol **(b)** x=5 mmol, y=10 mmol **(c)** x=7.5 mmol y=7.5mmol **(d)** x=15mmol, y=0 mmol **(e)** x=0 mmol, y=15mmol.

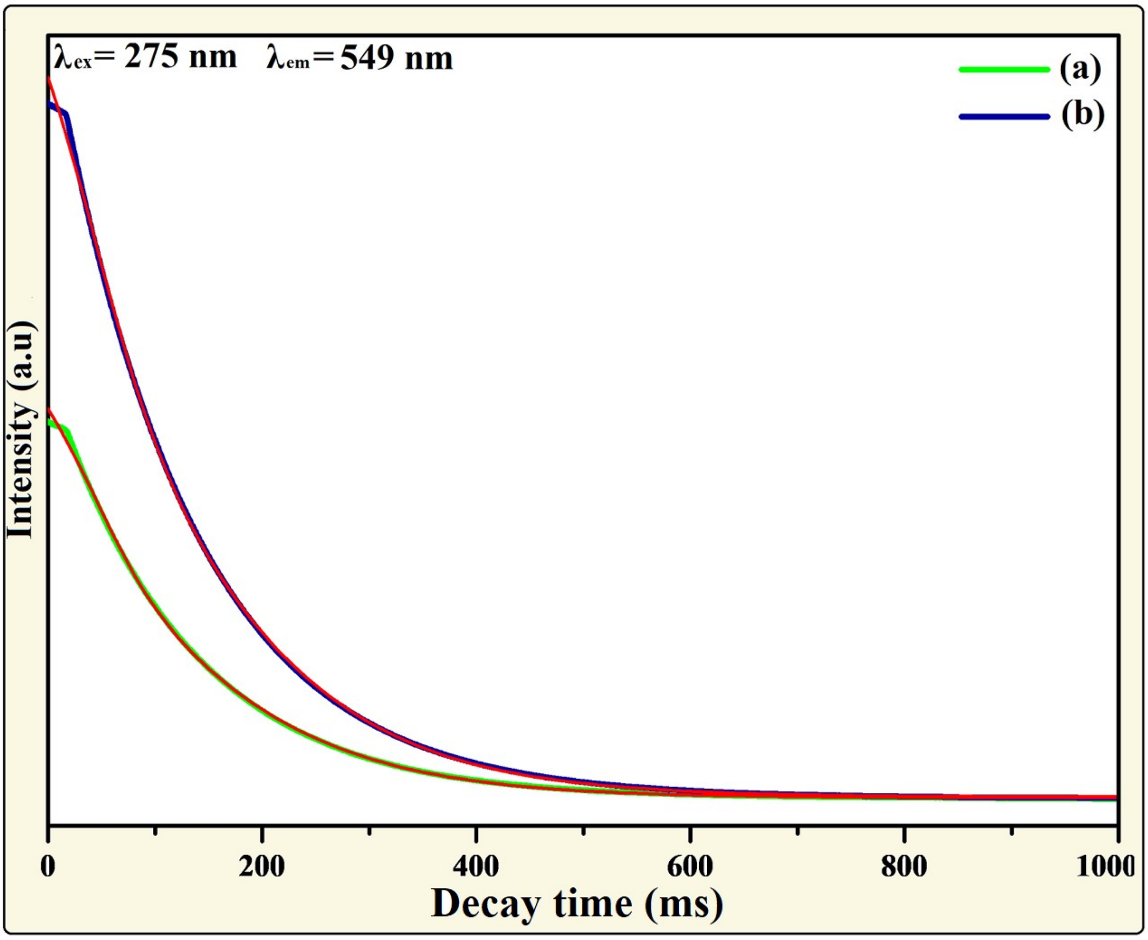

Fig. S7†: ESI Photoluminescence lifetime decay curves of as synthesized nanostructure

(a) $Na_xLi_yGdF_4:Tb^{3+}$ nanophosphors.

(b) $Na_xLi_yGdF_4:Tb^{3+}$@PMA@Phen@GO nanocomposite.

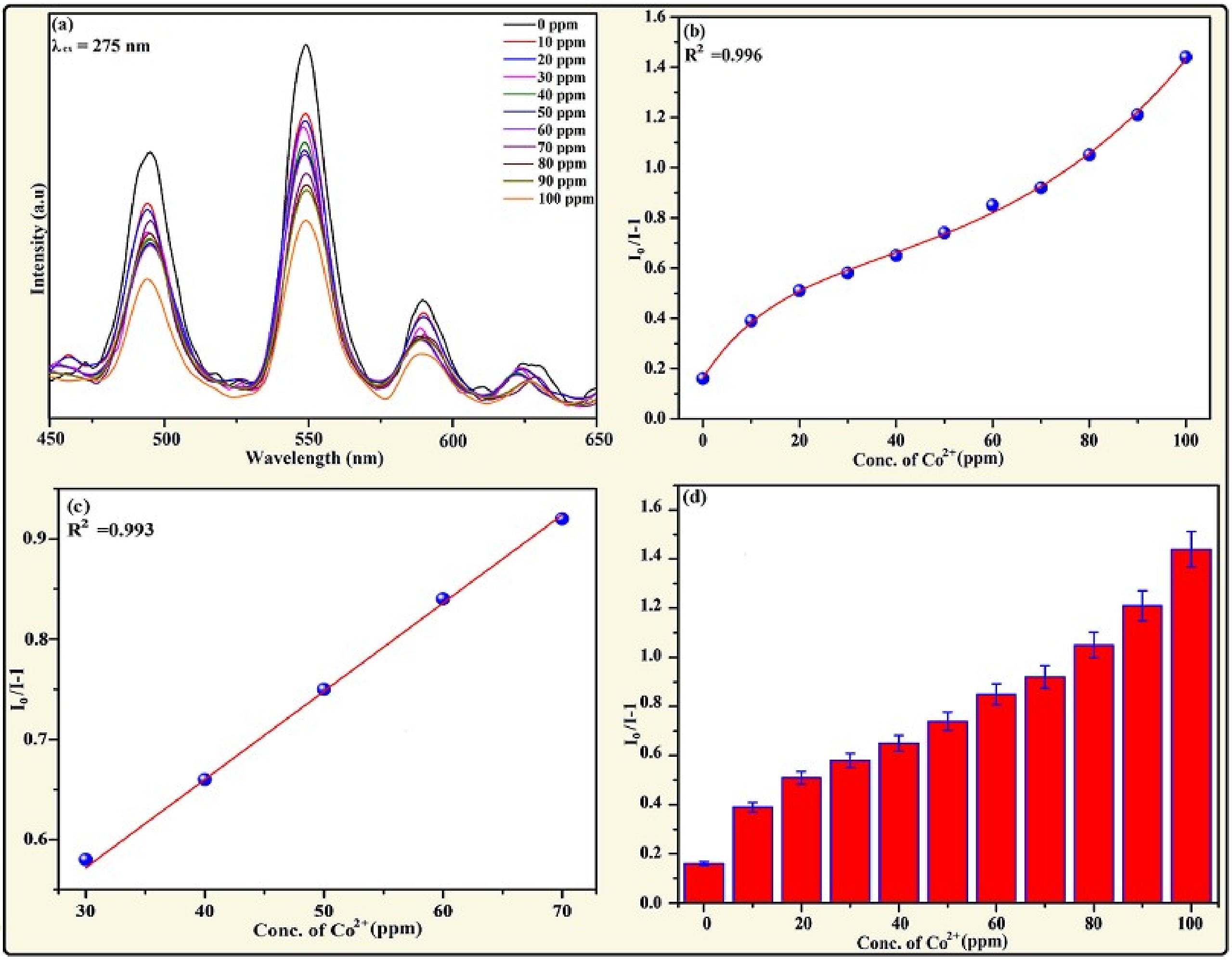

Fig. S8†: ESI Variation in photoluminescence intensity of designed chemosensor in presence of different Co^{2+} concentrations (from 0 to 100 ppm) selective excitation at λ_{ex} = 275 nm: (a) Emission spectra of nanophosphors with addition of Co^{2+} ion (using water as solvent) (b) Nonlinear Stern-Volmer plot of I_0/I-1 versus (Co^{2+}) concentrations (c) linear Stern-Volmer fitting and (d) Error bar

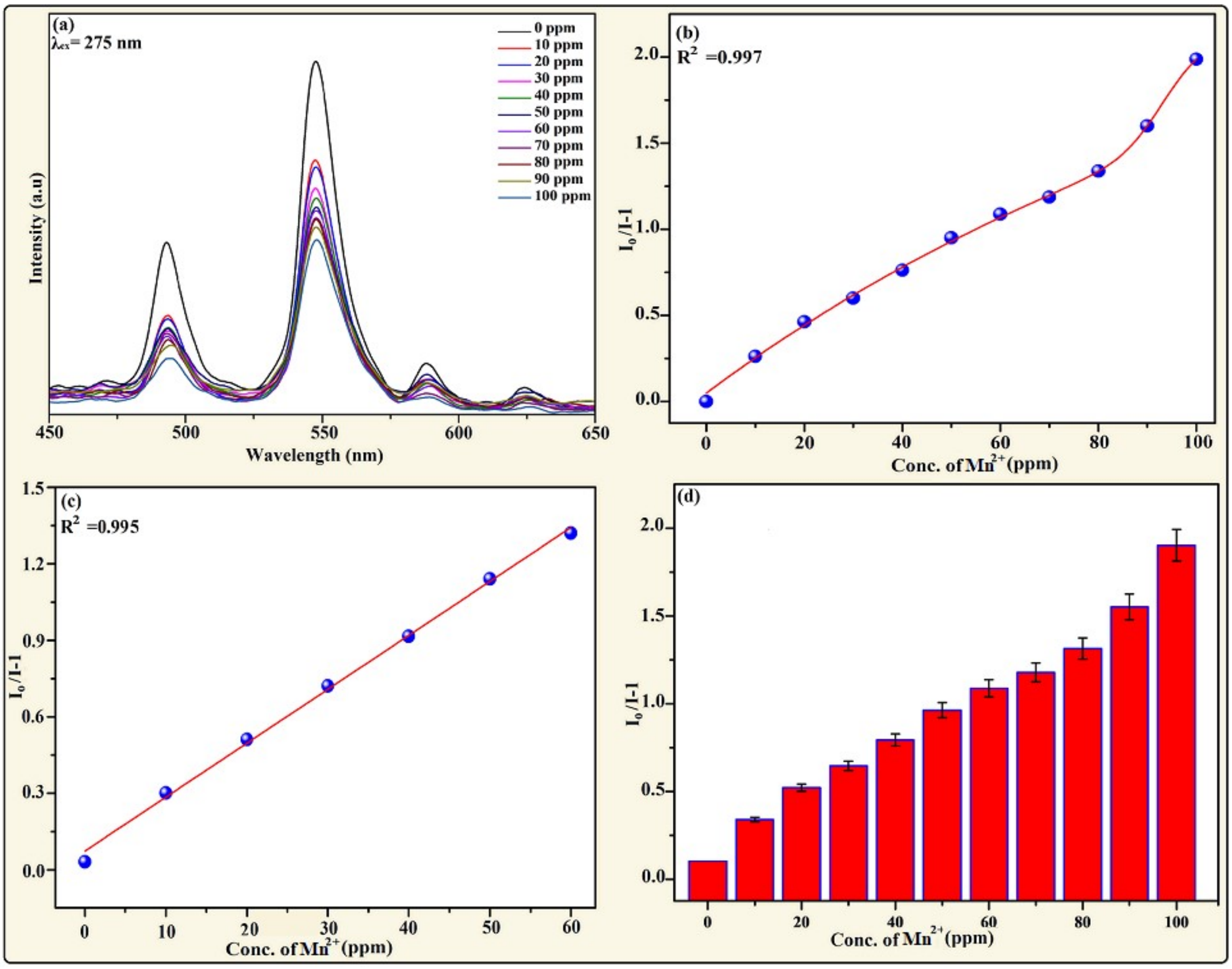

Fig. S9†: ESI Variation in photoluminescence intensity of designed chemosensor in presence of different Mn^{2+} concentrations (from 0 to 100 ppm) selective excitation at λ_{ex}= 275 nm (a) Emission spectra of nanophosphors with addition of Mn^{2+} ion (using water as solvent) (b) Nonlinear Stern-Volmer plot of I_0/I-1 versus (Mn^{2+}) concentrations (c) linear Stern-Volmer fitting and (d) Error bar

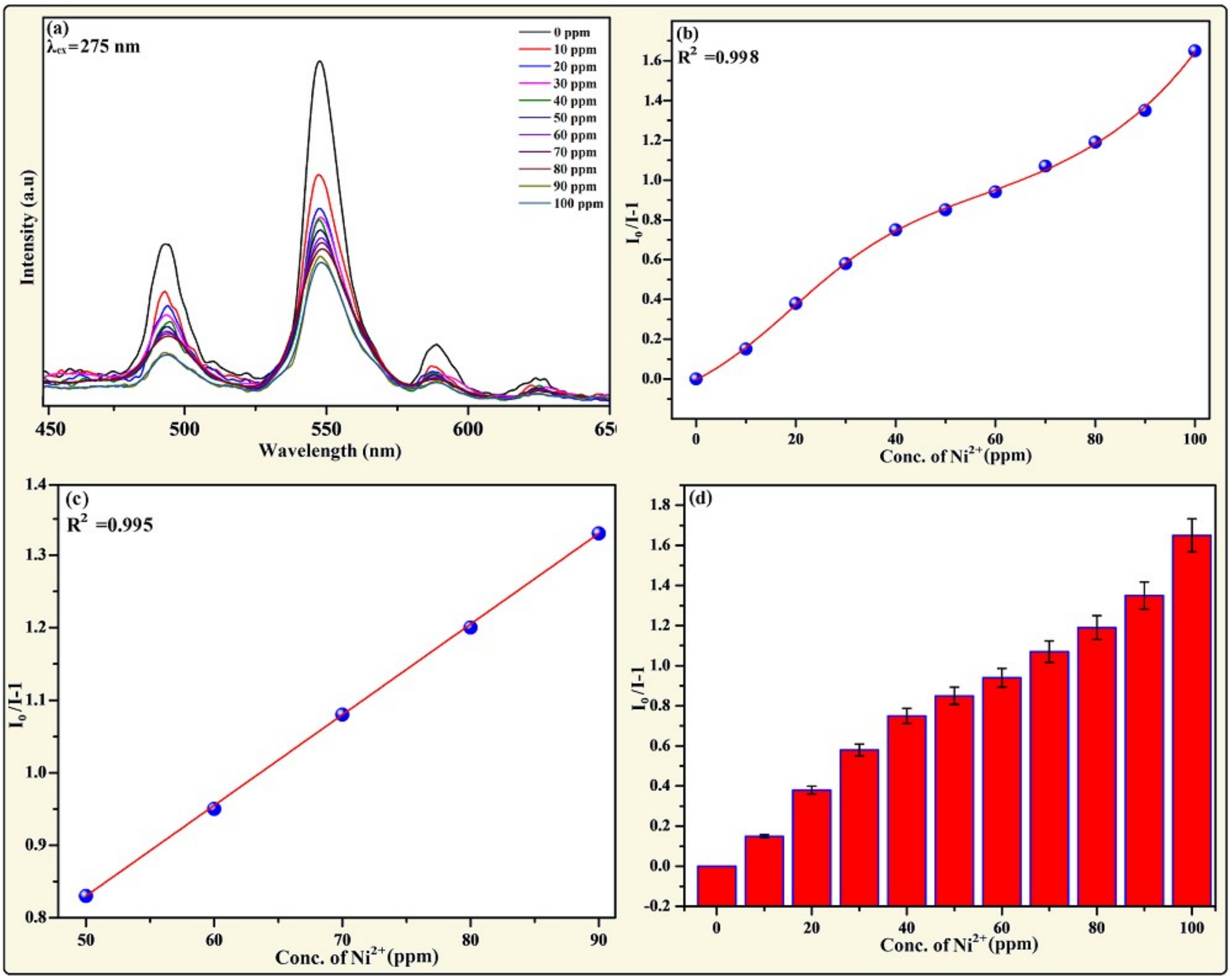

Fig. S10†: ESI Variation in photoluminescence intensity of designed chemosensor in presence of different Ni^{2+} concentrations (from 0 to 100 ppm) selective excitation at λ_{ex}= 275 nm (a) Emission spectra of nanophosphors with addition of Ni^{2+} ion (using water as solvent) (b) Nonlinear Stern-Volmer plot of I_0/I-1 versus (Ni^{2+}) concentrations (c) linear Stern-Volmer fitting and (d) Error bar

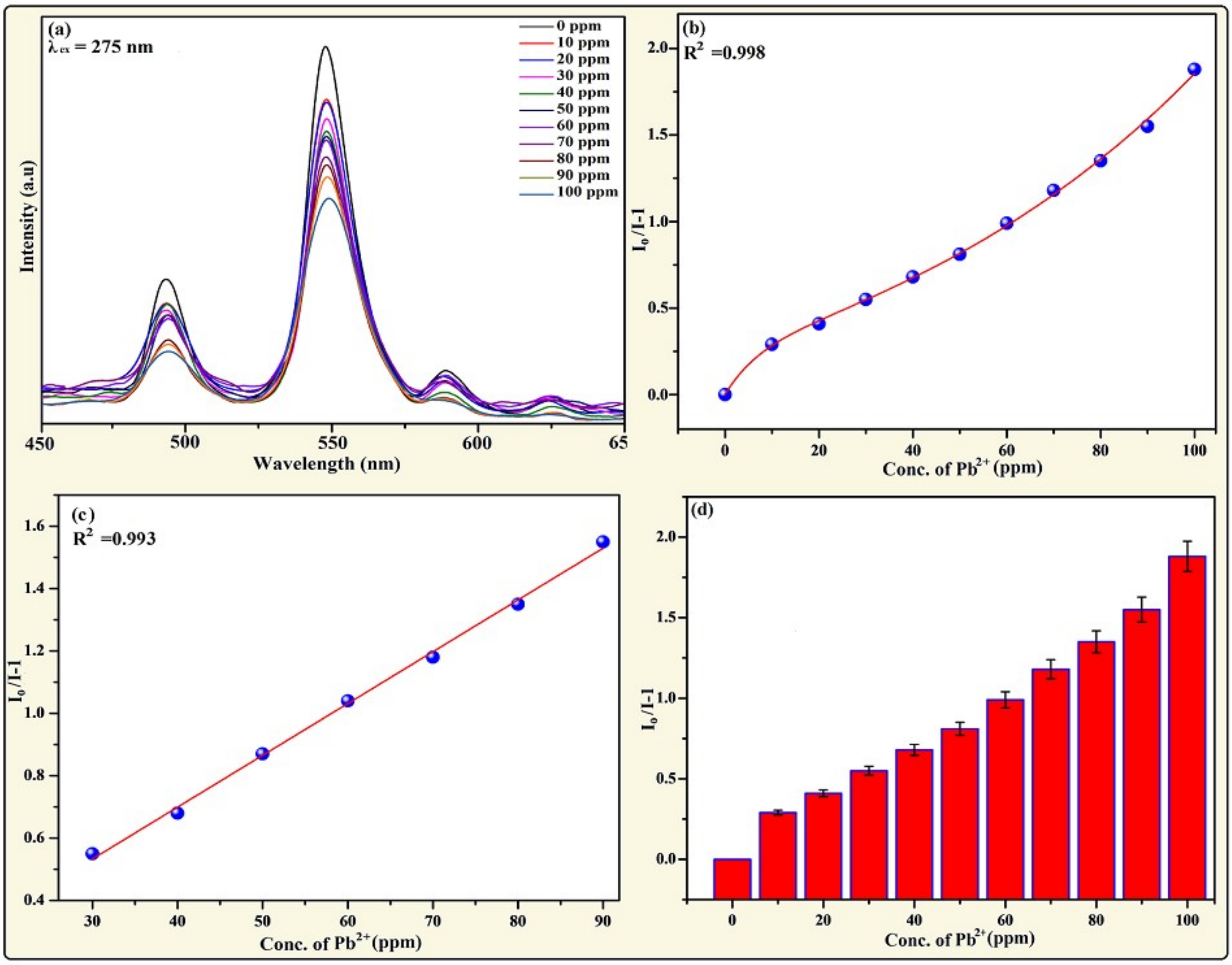

Fig. S11†: ESI Variation in photoluminescence intensity of designed chemosensor in presence of different Pb^{2+} concentrations (from 0 to 100 ppm) selective excitation at λ_{ex} = 275 nm: (a) Emission spectra of nanophosphors with addition of Pb^{2+} ion (using water as solvent) (b) Nonlinear Stern-Volmer plot of $I_0/I-1$ versus (Pb^{2+}) concentrations (c) linear Stern-Volmer fitting and (d) Error bar

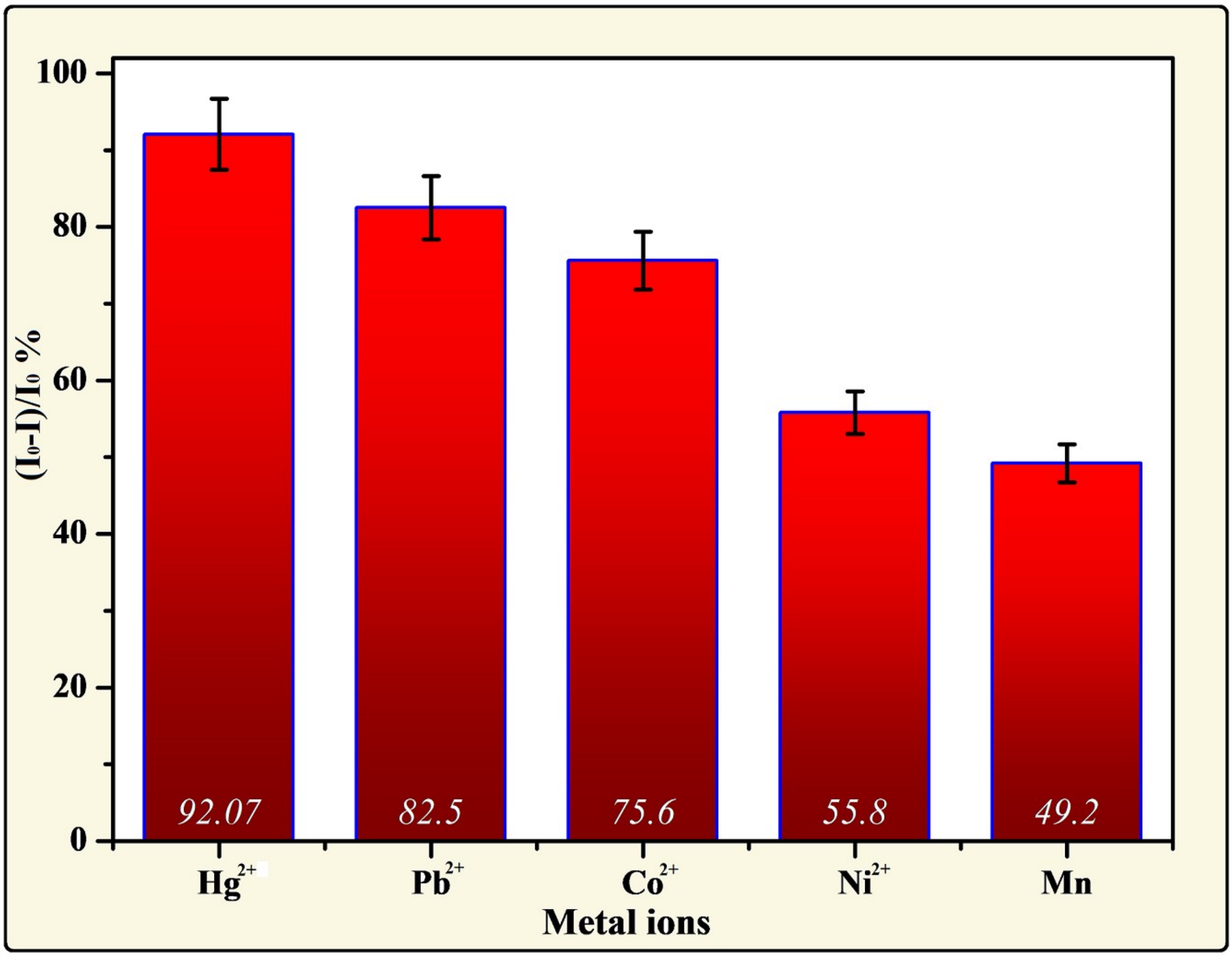

Fig. S12†: ESI Quenching efficiency of the prepared nanosensor in presence of different metals ions analytes (100 ppm) in aqueous medium.

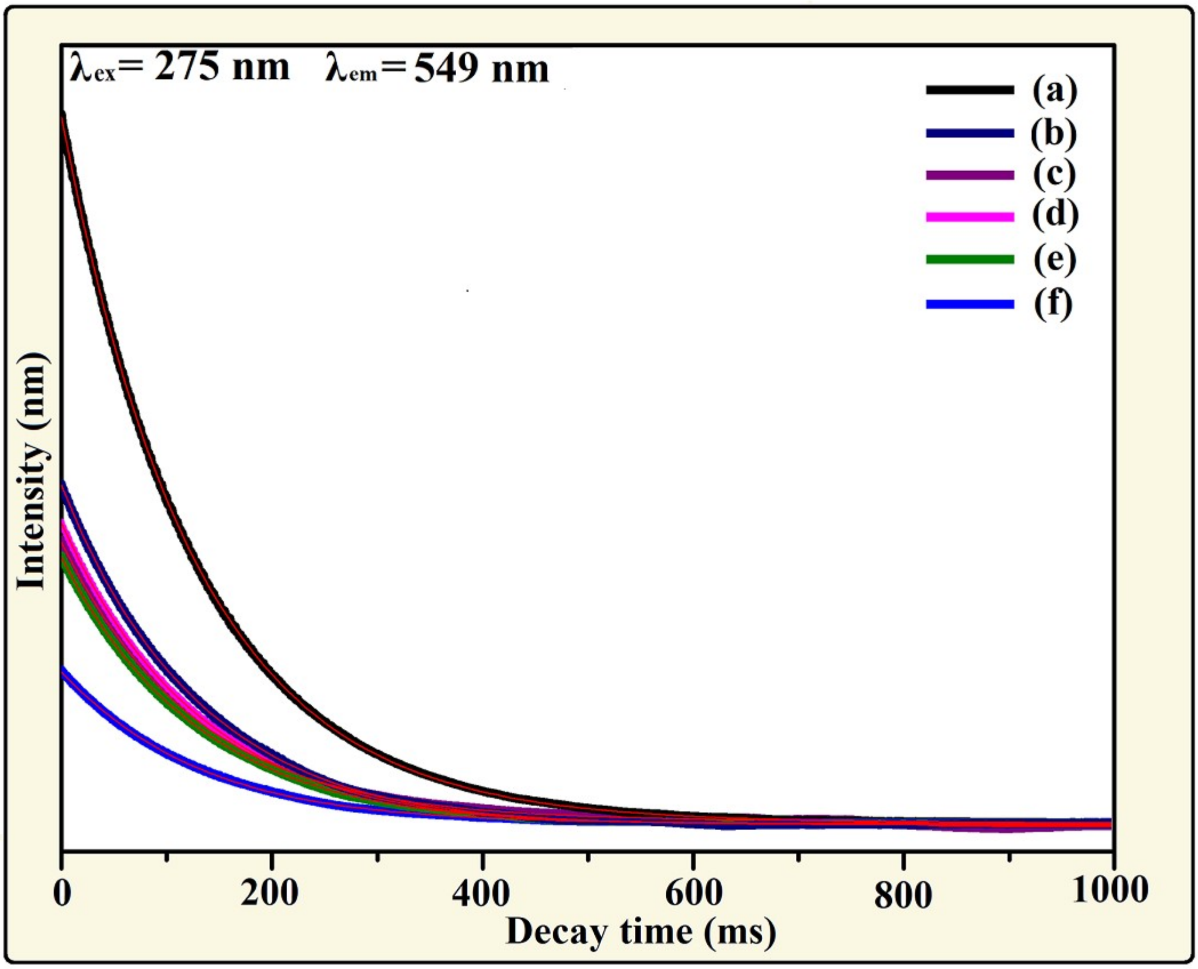

Fig. S13†: ESI Photoluminescence lifetime decay curves of as-fabricated nanosensor with addition of various toxic metal ions **(a)** blank nanosensor without addition of mrtal analyte **(b)** nanosensor with addition of Mn^{2+} (100 ppm) **(c)** nanosensor with addition of Ni^{2+} (100 ppm) **(d)** nanosensor with addition of Co^{2+}(100 ppm) **(e)** nanosensor with addition of Pb^{2+} (100 ppm) **(f)** nanosensor with addition of Hg^{2+}(100 ppm)

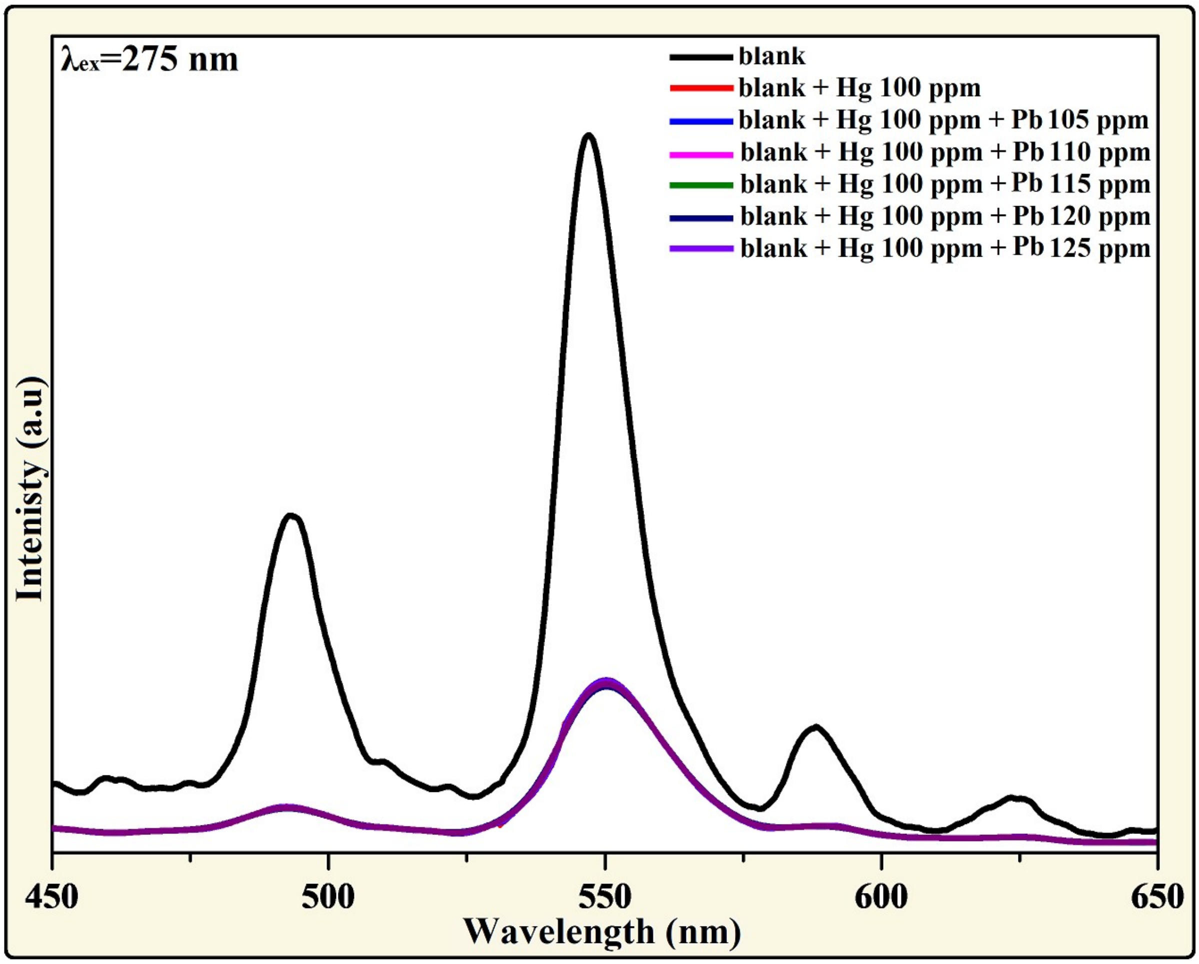

Fig. S14†: ESI Photoluminescence emission spectra of as-designed nanosensor with the addition of Hg^{2+} ion and different concentrations of Pb^{2+} ion.

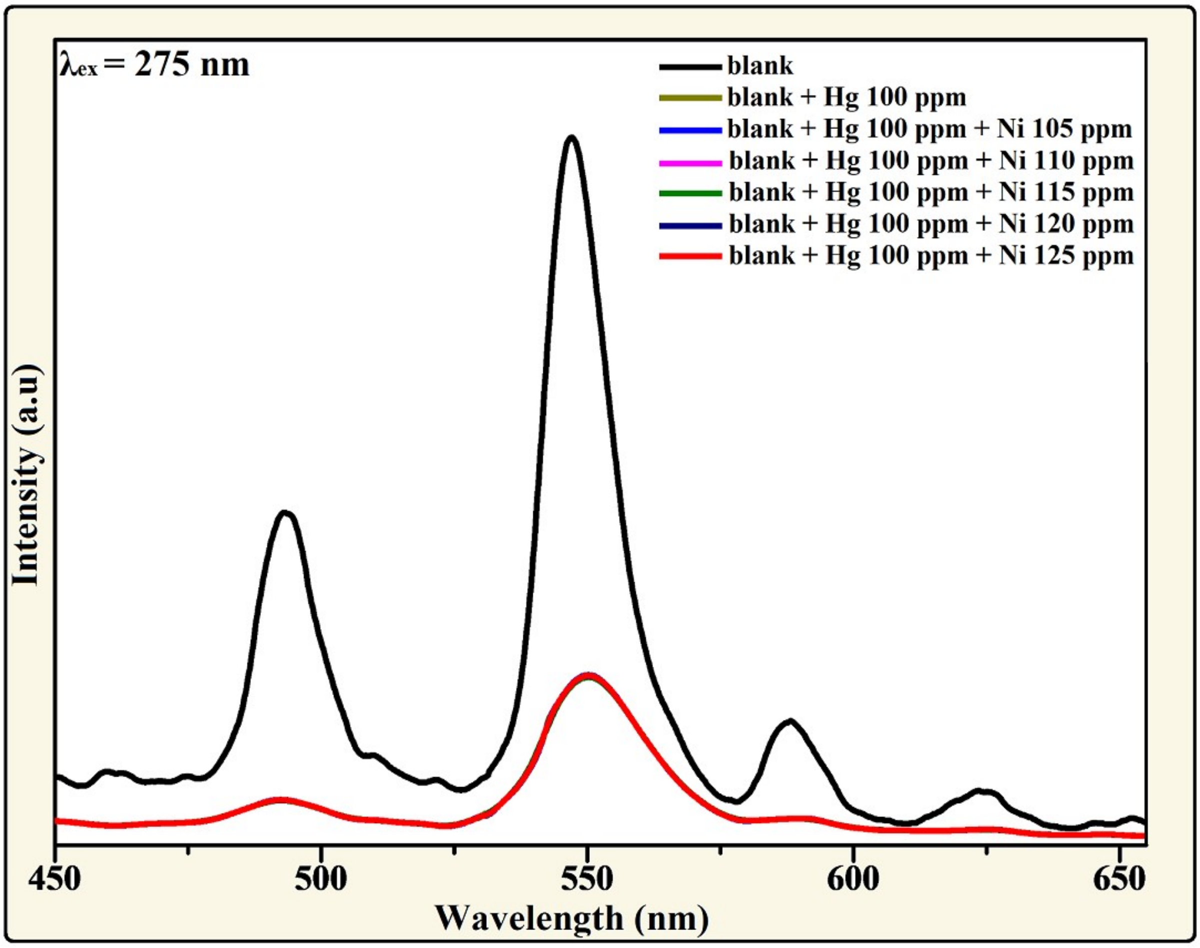

Fig. S15†: ESI Photoluminescence emission spectra of as-designed nanosensor after the addition of Hg^{2+} ion along with different concentrations of Ni^{2+} ion.

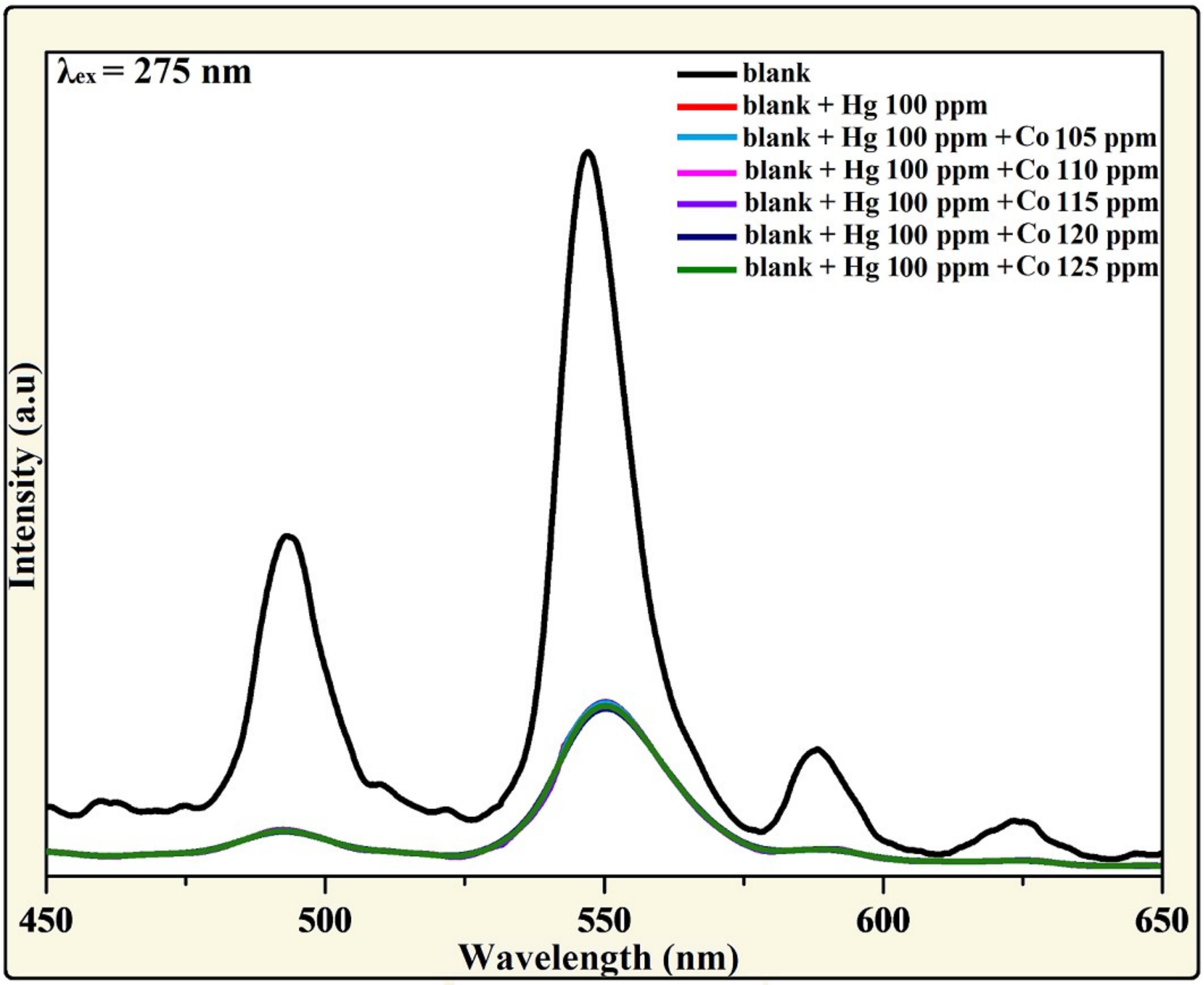

Fig. S16†: ESI Photoluminescence emission spectra of as-designed nanosensor with the addition of Hg^{2+} ion and different concentrations of Co^{2+} ion.

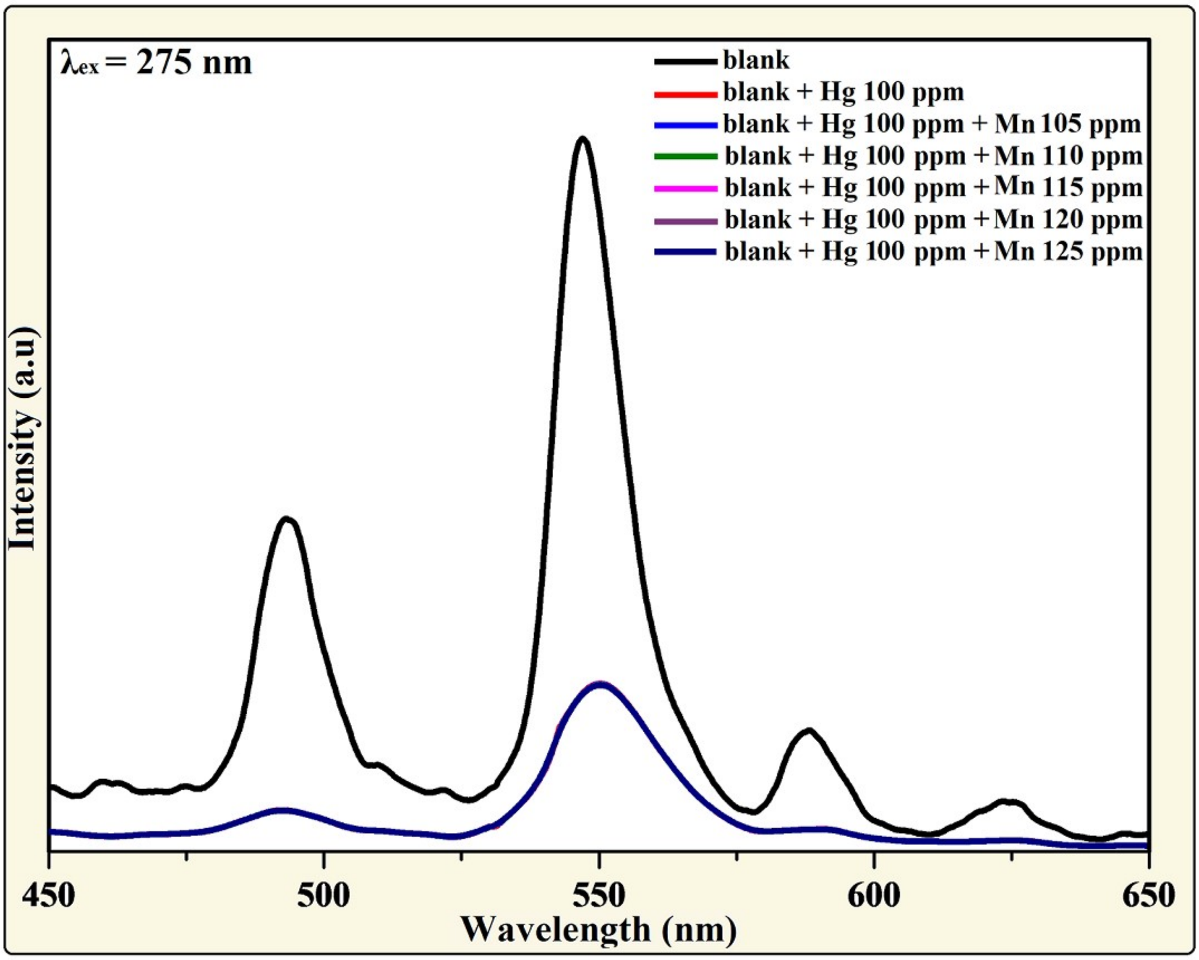

Fig. S17†: ESI Photoluminescence emission spectra of as-designed nanosensor with the addition of Hg^{2+} ion and different concentrations of Mn^{2+} ion.

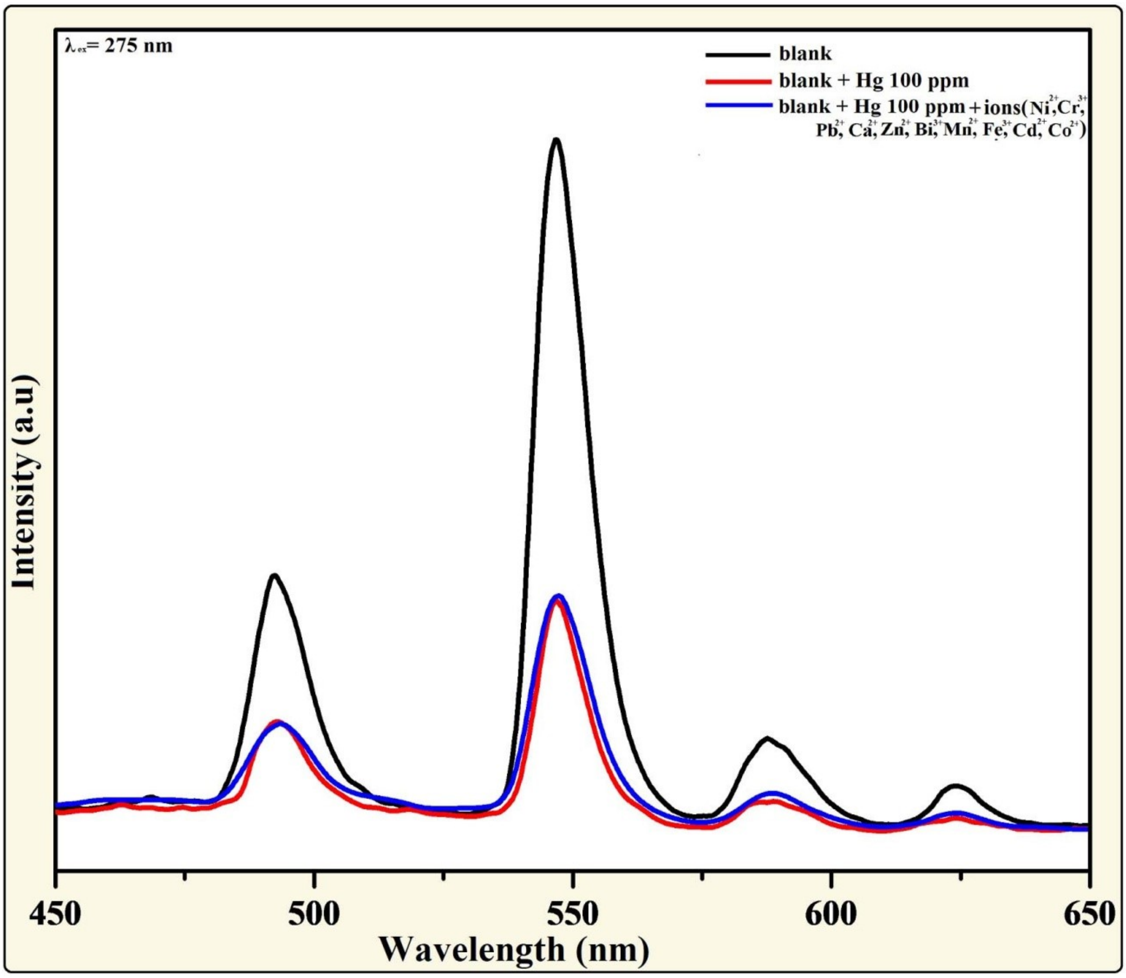

Fig. S18†: ESI Photoluminescence emission spectra of as-designed nanosensor with the addition of Hg^{2+} ion and presence of different metal ions.